

Agricultural intensification vs climate change: What drives long-term changes of sediment load?

5 Shengping Wang^{1,2,3*}, Peter Strauss², Carmen Krammer², Elmar Schmaltz²,
Borbala Szeles^{3,4}, Günter Blöschl^{3,4}

1. College of Hydraulic and Hydro-Power Engineering, North China Electric Power University, Beijing, 102206, P.R. China

2. Institute for Land and Water Management Research, Federal Agency for Water Management, A-3252 Petzenkirchen, Austria

10 3. Institute of Hydraulic Engineering and Water Resources Management, Vienna University of Technology, Vienna, Austria

4. Vienna Doctoral Programme on Water Resource Systems, Vienna University of Technology, Vienna, Austria

***Corresponding author:** Shengping Wang

Email: wangshp418@126.com; Shengping_Wang@ncepu.edu.cn

15

Abstract: Climate change and agricultural intensification are expected to increase soil erosion and sediment production from arable land in many regions. However, so far, most studies were based on short-term monitoring and/or modeling, making it difficult to assess their reliability in terms of estimating long-term changes. We present the results from a unique data set consisting of measurements of sediment loads from a 60ha catchment (the Hydrological Open Air Laboratory, HOAL, in Petzenkirchen, Austria) over a time period spanning 72 years. Specifically, we compare Period I (1946-1954) and Period II (2002-2017) by fitting sediment rating curves for the growth and dormant seasons for each of the periods. The results suggest a significant increase in sediment loads from Period I to Period II with an average of

20

25

$11.6 \pm 10.8 \text{ ton}\cdot\text{yr}^{-1}$ to $63.6 \pm 84.0 \text{ ton}\cdot\text{yr}^{-1}$. The sediment flux changed mainly due to a shift of the sediment rating curves (SRC), given that the mean daily discharge significantly decreased from $5.0 \pm 14.5 \text{ l}\cdot\text{s}^{-1}$ for Period I to $3.8 \pm 6.6 \text{ l}\cdot\text{s}^{-1}$ for Period II.

30 The slopes of the SRC for the growing season and the dormant season of Period I were 0.3 and 0.8, respectively, whilst they were 1.6 and 1.7 for Period II, respectively. Climate change, considered in terms of rainfall erosivity, was not responsible for this shift, given that erosivity decreased by 30.4% from the dormant season of Period I to that of Period II, and no significant difference was found between the growing
35 seasons of Periods I and II. However, the change in sediment flux can be explained by the changes in crop type and parcel structure. At low and median streamflow conditions, land consolidation in Period II (*i.e.* the parcel effect) had no apparent influence on sediment production. Whilst with increasing stream flow, parcel structure became more important in controlling sediment yield, as a result of an enhanced
40 sediment connectivity in the landscape, leading to a dominant role at high flow conditions. The increase in cropland between Periods I and II at the expense of grassland led to an increase in sediment flux, although its relevance was surpassed by the effect of parcel structure change at high flow condition. We conclude that both land cover change and land consolidation should be accounted for when assessing
45 sediment flux changes. Especially during high flow conditions, parcel structure change substantially alters sediment fluxes, which is most relevant for long-term sediment loads and land degradation. Increased attention to improving parcel structure is therefore needed in climate adaptation and agricultural catchment management.

50 **Keywords: Sediment regime; Land use/cover change; Parcel structure;**
Climate change; Agricultural catchment

Introduction

Soil erosion is a phenomenon of worldwide importance because of its environmental
55 and economic consequences (García-Ruiz, 2010; Prosdocimi et al., 2016). Climate
change, land use/cover changes and other anthropogenic activities are commonly
considered potential agents that drive variation of soil erosion rates (Nearing et al.,
2004; Zhang et al., 2021). The impacts of climate change (e.g. Nearing et al., 2004;
Zhang and Nearing., 2005; Mullan, 2013; Palazon and Navas, 2016) and of land use
60 and cover change (LUCC) (e.g. Bochet et al., 2006; Korkanç et al., 2018; Nampak et
al., 2018; Li et al., 2019; Perović et al., 2018) on erosion have been studied in recent
years. As the two agents usually exert their influence on soil erosion simultaneously,
their relative contributions have also been increasingly investigated in recent years
(e.g. Bellin et al., 2013; Sun et al., 2020; Zhang et al., 2021). Combining field
65 investigations with model simulations, Zhang et al. (2021) quantitatively evaluated
the contributions of climate change, land use and silt trap dams to the reduction of
sediment load of a typical Loess watershed over 1987-2016, with the contribution
values being +29%, +40%, and +31%, respectively. Scholz et al.(2008) modelled how
management practices on the local scale will affect soil erosion compared to climate
70 change. They found that the conservational management practices had a greater

impact on erosion than climate change. Also, livestock grazing accelerated soil erosion was found to be more important than climate change in the Qinghai-Tibet Plateau (Li et al., 2019).

The previous findings provide valuable information on understanding how LUCC and
75 climate change affect soil erosion and sediment load. However, it seems that most of the previous studies considered LUCC and landscape structure change together. The relevance of landscape structure changes alone has so far received less attention, even though land-use policies, such as land consolidation, have changed agricultural practices to a large extent since 1945, the beginning of agricultural industrialization
80 (e.g. Moravcová et al., 2017; Devaty et al., 2019), and in particular in countries where the industrialization of agriculture is relatively recent (Bouma et al., 1998; Moravcova et al., 2017; Zhang et al., 2021).

Landscape structures usually influence erosion due to the boundary effects between land uses and land units (parcels) that differ in water and sediment trapping capacity
85 (Baudry and Merriam, 1988; Merriam, 1990; Takken et al., 1999; Phillips et al., 2011).

Van Oost et al. (2000) and Devaty et al. (2019) evaluated the role of landscape structure by accounting for its spatial connectivity using modelling approaches and found that landscape structure is an essential factor when assessing the risk of soil erosion affected by land use changes. Both studies emphasized the potential impacts
90 of parcel structure changes on sediment production through altering hydrological and sediment connectivity. However, both studies relied on models, making connectivity assumptions in their studies. Instead of focusing on the spatial connectivity, others

(e.g. Bakker et al., 2008; Sharma et al., 2011; Chevigny et al., 2014; Wang et al., 2021; Tang et al., 2021; Madarász et al., 2021) evaluated the effect of terrain, soil properties, lithology, management practices and other processes associated with landscape and/or land structure changes and highlighted their impact on sediment production. It has also been shown that the impact of landscape structure on erosion is more heterogeneous when different crops are grown, and the underlying lithology, soil properties and topography show substantial spatial variability across the catchment (David et al., 2014; Cantreul et al., 2020).

In our analysis, we evaluate the relative roles of climate change, LUCC and the change of land structure on sediment production, especially with a focus on understanding the respective role of LUCC and landscape structure change, based on long term observations that were not usually available in previous studies. We present the results from a unique data set consisting of measurements of sediment loads from a small agricultural catchment over a time window of 72 years. The study catchment is the 66 ha Hydrological Open Air Laboratory (HOAL) Petzenkirchen (Blöschl et al., 2016), which, in addition to being exposed to climate change, has experienced a significant change in land use and land cover as well as parcel structure due to altered land management policies during the past decades. Both discharge and suspended sediment concentration have been monitored in the HOAL catchment since the 1940s. This provides an opportunity to disentangle the impacts of parcel structure change, land use/land cover change, and climate change based on long-term measurements. Specifically, we aim at i) exploring how the sediment regime shifted between the

periods of 1946-1954 and 2002-2017; ii) analyzing whether climate change or land use changes (or both) were responsible for any change in the sediment regime; and iii) identifying the relevance of land structure change (i.e. land consolidation) on erosion control compared to that of a change in land use or cover.

2. Methods

2.1 Catchment characteristics

The HOAL catchment is situated in Lower Austria's alpine forelands (48°9' N, 15°9' E) with elevations ranging from 268 m to 323 m a.s.l. and a size of 66 ha (Figure 1). The climate of the catchment belongs to the temperate, continental climate zone (Dfb) according to Köppen-Geiger (Kottek et al., 2006), with a mean annual precipitation of 746 mm (1946 - 2006), 62% of the rain falling between May and October. The mean daily air temperature is 8.8°C (1946-2006), and the dominant land use is arable land, accounting for, on average, 82% of the catchment over the past few years. Typical crops include winter wheat, corn and barley. Deciduous trees grow along the stream (6%), 10% of the area is grassland, and 2% is paved. The subsurface of the catchment consists of tertiary marine sediments. Soils are classified into five types: calcic cambisols, vertic cambisols, gleyic cambisols, planosols and gleysols (IUSS Working Group WRB, 2015).

2.2 Data availability

Both discharge (Q , l/s) and suspended sediment concentration (C , mg/l) have been measured at the catchment outlet since the 1940s. A data set of discharge and sediment concentration was available for the period 1945-1954. After that,

measurements were stopped and started again in 1990. Therefore, data records for the period 1946-1954 (Period I) and 2002-2017 (Period II) were used for this analysis. To our knowledge, for the time period 1945-1954, almost no sediment concentration data are available in Austria, we therefore think that this database from the HOAL is extremely valuable and relevant for climate impact analysis. In Period II, the stream gauge was relocated. However, the difference in catchment size is very small (around 200 m²), and indicated by the different locations of the discharge gauge in Figure 1.

Due to technological advances, the measurement method of both Q and C changed between the two periods. In Period I, discharge was registered at 10 min resolution by a Thompson weir and a paper chart recorder, while in Period II, it was registered at 5 min resolution by an H-Flume and a pressure transducer. Sediment concentrations were measured manually every 3-4 days in Period I, whilst an automatic method (*i.e.* equal-discharge-increment sampling) plus additional manual sampling was applied in Period II. Daily precipitation and 5-min rainfall intensities were available for both periods, but for Period I, 5-min rainfall intensities were only available during the growing season.

We used parcel-based land use data from 1946 to 1949 and 2007 to 2012, representing Period I and Period II land use, respectively. Land use categories were agricultural land, including crop type, grassland, forest, roads and settlements (*i.e.* paved area). We defined a parcel as a continuous area of land with a single crop type. Parcel boundaries were specified according to the cadastral map and aerial photographs. In Period II, these boundaries were also visually inspected. Figure 1 depicts the

geographic catchment location, and parcel structure and land use for a specific year in each period.

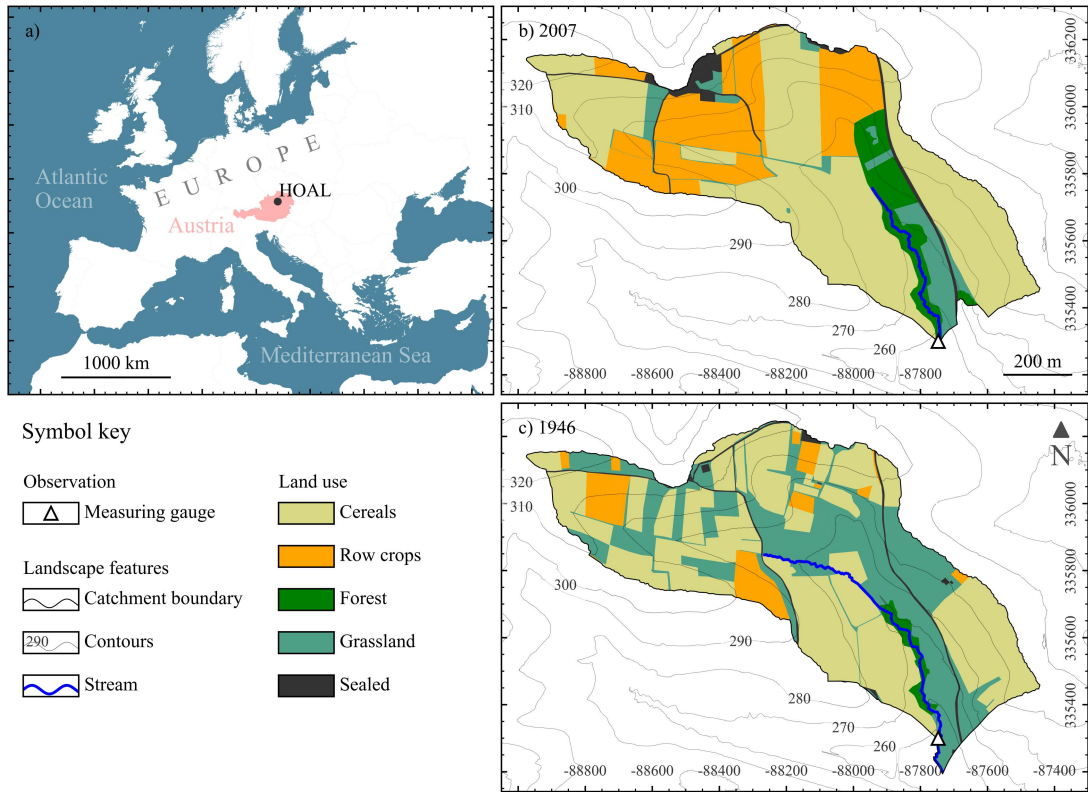


Figure 1 Geographical location of the HOAL catchment in Petzenkirchen in Austria and Europe (a) and Parcel structure and land use in the HOAL catchment for 2007 (b) and 1946 (c). Coordinates as EPSG: 31256 – MGI / Austria GK East (meters).

2.3 Data analysis

2.3.1 Changes in rainfall erosivity and flow regime

The erosive potential of rainfall events was quantified by the R-factor of the Revised Universal Soil Loss Equation (RUSLE), which is defined as the product of kinetic energy of a rainfall event and its maximum 30-min intensity, using the rainfall

erosivity tool RIST (USDA-Staff, 2019) according to

$$EI_{30} = \sum_{i=1}^m E_i \cdot I_{30,i} \quad (1)$$

where EI_{30} is the Annual R-factor (MJ*mm/ha*hr) calculated as the sum of single event R-factors, E_i is the total kinetic energy for a single event ($\text{kJ}\cdot\text{m}^{-2}$), I_{30} is the maximum rainfall intensity in 30 minutes within a single event ($\text{mm}\cdot\text{h}^{-1}$), and m is the number of events per year.

We assumed erosivity density ED (*i.e.* EI_{30} divided by event precipitation) to be a particularly relevant climatic indicator of soil erosion process and catchment sediment yield, because it is calculated as a combination of rainfall kinetic energy and maximum rainfall intensity of rain events. These are commonly considered as the relevant parameters of rain to trigger soil erosion. We, thus, tested whether the means of the monthly erosivity density (ED) are significantly different between Period I and Period II by using a t-test. Due to the absence of rainfall intensity measurements, we could not directly calculate ED for the months of the dormant season (November to March) of Period I. Instead, we calculated ED from a relationship between EI_{30} and monthly rainfall of Period II, assuming that the relationship was sufficiently temporally invariant over the investigated periods. Erosivity density is very low during the dormant season. The mean ED was 0.66 ± 0.21 and $2.54 \pm 2.43 \text{ MJ ha}^{-1} \text{ hr}^{-1}$ respectively for the dormant season and the growing season of Period I, whilst it was 0.42 ± 0.11 and $1.87 \pm 1.35 \text{ MJ ha}^{-1} \text{ hr}^{-1}$ respectively in Period II (Figure 3a). Thus, the error arising from the use of this relationship is expected to be small.

We also compared daily flow duration curves to understand whether hydrological regime change has influenced flow transporting capacity and sediment regime change.

Following the definitions of Smakhtin (2001), we compared low flow ($Q_{70\%}$), high flow ($Q_{10\%}$) and median flow rate ($Q_{50\%}$) quantiles for the two periods.

200 2.3.2 Sediment regime analysis

We first estimated sediment load for the different time periods. Daily mean streamflow or daily mean sediment concentration were estimated as arithmetic average of multiple observations within a day, and then we estimated sediment load for each month according to equation (2):

$$205 \quad Y = \sum_i \left(\frac{(\bar{Q}_{i-1} + \bar{Q}_i)}{2} * \frac{(\bar{C}_{i-1} + \bar{C}_i)}{2} * T_i * 0.0864 \right) \quad (2)$$

where Y is the sediment load for a month ($\text{kg} \cdot \text{mon}^{-1}$), \bar{Q}_i and \bar{C}_i are mean daily discharge ($\text{l} \cdot \text{s}^{-1}$) and mean daily sediment concentration ($\text{mg} \cdot \text{l}^{-1}$), respectively, for a specific day i having data records; \bar{Q}_{i-1} and \bar{C}_{i-1} are mean daily discharge ($\text{l} \cdot \text{s}^{-1}$) and mean daily sediment concentration ($\text{mg} \cdot \text{l}^{-1}$), respectively, for the previous day with
210 available data measurements as well; $T_i (s)$ is the elapsed time between day i and the last previous recording day. The latter value depends on how often sediment concentration was recorded within a month. The statistical differences of sediment loads between seasons and between periods were examined by a t-test.

Sediment regimes are usually analyzed using sediment rating curves (SRC).

215 Following a common approach (Asselman, 2000; Warrick and Rubin, 2007; Sheridan et al., 2011; Vaughan et al., 2017; Khaledian et al., 2017), the SRCs were here assumed to follow a power-law function, which was fitted by least squares regression:

$$C = a \cdot Q^b \quad (3)$$

where C is sediment concentration ($\text{mg} \cdot \text{l}^{-1}$), Q is discharge ($\text{l} \cdot \text{s}^{-1}$), and a and b are

220 regression coefficients. The coefficient a is usually associated with easily transported intensively weathered materials and may vary over seven orders of magnitude (Syvitski et al., 2000). The parameter b represents the capacity of the stream to erode and transport sediment, reflecting how sediment concentration is non-linearly related to streamflow (Sheridan et al., 2011; Fan et al., 2012). It typically varies from 0.5 to 225 1.5 and rarely exceeds 2. Sometimes b is also regarded as a measure of the quantity of new sediment sources available (Vanmaercke et al., 2010; Guzman et al., 2013).

Considering that data records were registered with different temporal resolutions for Periods I and II (See section 2.2), for the sake of consistency, we used monthly averages, as in other studies (Syvitski and Alcott, 1995; Sheridan et al., 2011; Hu et al., 230 2011), to construct SRC. We assumed that monthly averages could reflect a varied hydrological and/or sediment response to seasonally prevailing weather characteristics such as dry periods or convective storms (Sheridan et al., 2011).

We chose arithmetic means of the observations to represent the monthly Q and C values. These monthly averages were pooled together and then grouped into growing 235 season of Period I (Period I_G), dormant season of Period I (Period I_D), growing season of Period II (Period II_G), and dormant season of Period II (Period II_D), respectively. For each of these four periods, we fitted SRC.

We analyzed the fitted SRC by two strategies to evaluate whether and how the sediment regime changed between these periods. Besides directly comparing the 240 slopes of the four seasonal SRCs by ANCOVA analysis, we also fitted the SRC for each specific year's season and plotted the regression coefficients a against their

corresponding b to evaluate a possible sediment regime shift during Periods I and II.

The latter framework was adapted from Thomas (1988), and also employed by

Asselman et al. (2000) and Fan et al. (2012) to examine differences in sediment

245 regimes between spatially different sites. Also Sheridan et al. (2011) used the
framework to reveal post-fire temporal shifts of a sediment regime. Thomas (1988)
suggested that time-based sampling methods (either random sampling or systematic
sampling) preferentially use observations of relatively small discharges to fit a SRC,
tending to reduce the slope and increase the intercept of a SRC (see the point C in

250 Figure 2b); In contrast, flow-based automatic sampling methods such as
equal-discharge-increment sampling preferentially use observations of relatively large
discharges. Thus, they tend to cause a reversed pattern of a and b (*i.e.* increase the
slope and decrease the intercept of SRC, see the point A in Figure 2b). However,
irrespective of sampling practices, the pairs of data points a against b will likely be

255 allocated along a straight line, if sediment transport regimes are similar. The reason
for the a - b pairs lying nearly on a straight line is mainly due to a mathematical
property, that is, the slopes could be expressed by a linear function of the intercepts
with the coordinates of the common point (Thomas, 1988). Therefore, for years with
similar means of log- Q and log- C , the SRCs will pass through one common point O

260 (Thomas, 1988; Syvitski et al., 2000; Desilets et al., 2007; Sheridan et al., 2011). This
common point O (Figure 2a) is usually interpreted to reflect time invariant catchment
characteristics, such as relief, drainage area, and drainage density, while the variation
of the slope of SRCs (Figure 2a) is interpreted to reflect temporally dynamic

characteristics, such as average or maximum discharge and sediment availability

265 (Asselman, 2000). The coefficients a are usually inversely linearly related to b
(Thomas, 1988, Syvitski et al., 2000 and Desilets et al., 2007), and each point is
representative of a period (or a catchment). If sediment transport regimes are similar
between periods (catchments), the points will be plotted on the same line (such as A,
B, C in Figure 2b), with points A of Figure 2b (upper-left-side) often exhibiting
270 steeper sediment rating curves than points C (lower-right side). As for different lines
in Figure 2b, the lower ones characterized by points A', B', and C' represent situations
with most of the annual sediment load being transported at relatively low flow
discharges, whilst the higher ones characterized by A, B, and C represent situations
with suspended sediment being mainly transported at high streamflow. Compared to a
275 direct evaluation of rating curves, relating coefficient a to exponent b is more
conductive to revealing temporal evolution of sediment regime (Syvitski et al., 2000;
Desilets et al., 2007). The change in the relationship of coefficients a against b
between the periods was also examined by ANCOVA .

280

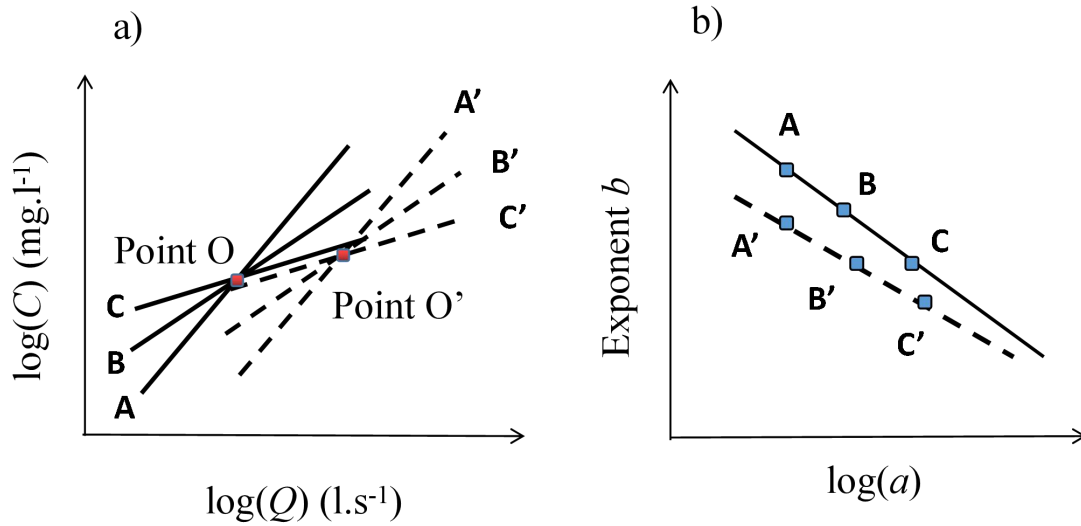


Figure 2 Schematic showing a) how sediment rating curves (SRC) may rotate around a common point and b) how exponents b of the SRC relate to coefficients a . Lines A, B and C on the left are SRC of different periods (e.g. years) sharing a similar common point O. Once sediment regimes shift due to the changes in catchment characteristics (change in drainage density, drainage area, and topography) the common point O would change to point O', and the linear relationship between a and b of the SRC would exhibit a shift as well. The schematic is based on $\log C = \log a + b \log Q$ (Equation 3).

To account for uncertainties of the fitted SRC during each period, we additionally established theoretical sediment rating curves (tSRC)

i) For each period (*i.e.* Period I_G, Period I_D, Period II_G, and Period II_D), we carried out random sampling of $\log a$ ($n=500$, package "sample" in RStudio), assuming that the samples of the coefficient of $\log a$ follow normal distributions, which was examined with a Kolmogorov-Smirnov test of normality (mean = 1.02, SD = 2.01, $n=44$, $p<0.05$);

ii) Given the set of the sampled 500 values of $\log a$, we generated a set of values b according to the previously established linear relationship between $\log a$ and b ;

iii) Given a set of specified Q values, we derived 500 tSRC for each period,

corresponding to the paired log a and b samples;

iv) Using these tSRC we calculated the 50 percentile, 5 percentile, and 95 percentile for each period to estimate the uncertainties of the sediment rating curves.

305 The tSRC of the periods were also used to quantify the effect of land consolidation, *i.e.* the change of parcels structure and sizes (Parcel_effect) and the effect of land use and land cover changes (LUCC_effect). Since vegetation usually plays a minor role in the dormant season due to the absence of a dense vegetation cover on arable land and little erosive rainfall (Madsen et al., 2014; Kundzewicz, 2012; Salesa and Cerda, 2020; 310 Hou et al., 2020), landscape structure in the dormant season was considered a dominant factor for water and sediment transfer across the land surface, and thus runoff production and sediment production (Sharma et al., 2011; Devátý et al., 2019). Therefore, we hypothesized that the total change in sediment yield (Total_effect) resulted from land cover change (LUCC_effect), land structure change (Parcel_effect) 315 and climate change (Climate_effect). Since the area of our catchment is only 0.67 km², no obvious change was found in the shape of the small stream for the two periods. Stream sediment resuspension is rather small (Eder et al., 2014), the contribution of bank erosion was not taken into account. The effects of land cover and land structure change was quantitatively separated according to the seasonal differences in tSRC 320 after determining the climate change effect. Specifically, we assumed that the shift of sediment regime from Period I_D to Period II_G was representative of the Total_effect (Equation 4), and the shift in sediment regime between Period I_D and

Period II_D was mainly due to land consolidation (Parcel_effect) (Equation 5). The LUCC effect, thus, could be estimated according to Equation (6) if the Climate_effect was insignificant (section 3.1). The contributions of Parcel_effect and LUCC_effect to the Total_effect were estimated according to Equations (7) and (8), respectively.

$$\text{Total_effect} = tSRC_{50\%}(\text{Period II_G}) - tSRC_{50\%}(\text{Period I_D}) \quad (4)$$

$$\text{Parcel_effect} = tSRC_{50\%}(\text{Period II_D}) - tSRC_{50\%}(\text{Period I_D}) \quad (5)$$

$$\text{LUCC_effect} = \text{Total_effect} - \text{Parcel_effect} - \text{Climate_effect} \quad (6)$$

$$\text{Parcel_effect (\%)} = \frac{\text{Parcel_effect}}{\text{Total_effect}} \times 100 \quad (7)$$

$$\text{LUCC_effect (\%)} = \frac{\text{LUCC_effect}}{\text{Total_effect}} \times 100 \quad (8)$$

3. Results

3.1 Changes in climate and flow regime

Because climate change is often found responsible for hydrological change (e.g., Kelly et al., 2016; Wang et al., 2020), we compared erosivity density (*ED*) and monthly precipitation (*P*) of the two periods to examine whether climate affected the variation of the sediment regime in the catchment (Figure 3). The mean monthly *ED* in the growing season were 2.37 ± 1.38 and 1.84 ± 0.86 MJ.ha⁻¹.hr⁻¹ for Periods I and II, respectively (Figure 3a). No significant difference ($p > 0.05$) was found between the two growing seasons. Mean monthly *ED* in the dormant seasons showed a significant ($p < 0.05$)

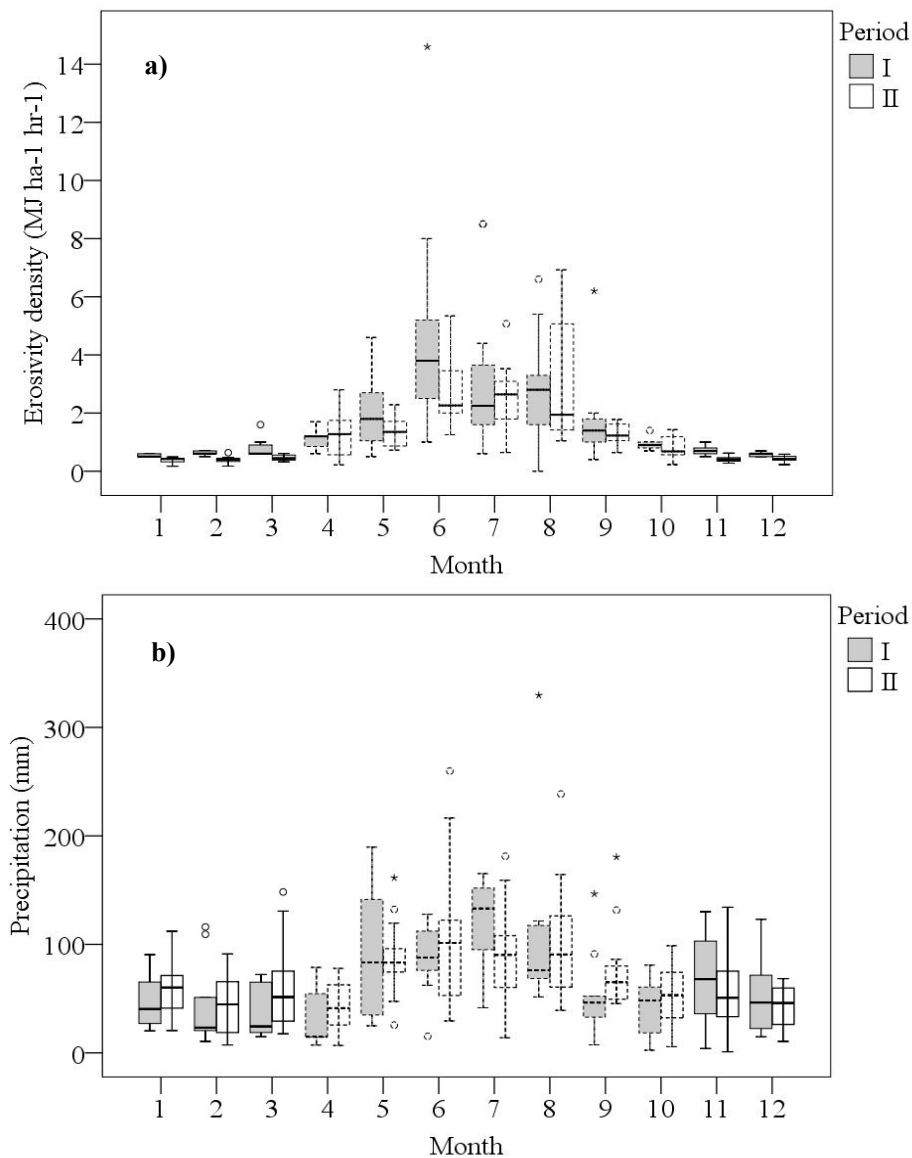


Figure 3 Monthly erosivity density a) and monthly precipitation b) for Periods I and II. The bars with a dashed outline represent the growing seasons (April to October), the bars with a solid outline the dormant seasons (November to March). The whiskers indicate the range between the minimum and the maximum, the asterisks indicate the outliers.

decrease from the first to the second period (0.66 ± 0.21 and 0.42 ± 0.11 ($\text{MJ} \cdot \text{ha}^{-1} \cdot \text{hr}^{-1}$), respectively). A *t*-test suggests that there was no significant ($p > 0.05$) difference in mean monthly P between the first and second periods in both the dormant and the

growing seasons (Figure 3b). The mean monthly P was 50 ± 33 and 76 ± 54 mm for
355 the dormant and growing season of Period I, and it was 53 ± 29 mm and 79 ± 47 mm
for the two seasons of Period II. The decrease in ED during the dormant season of
Period II and the insignificant change in monthly P suggest that climate change
between Period I and II was not responsible for an increased sediment load (see
section 3.3). It should be noted, that processes related to snow play a minor role in the
360 catchment because it is considered a lowland catchment, located in a region with very
small amounts of snowfall. Thus, a possible change in the proportion of snowfall in
precipitation during the winter season of Periods I and II was not accounted for when
addressing the impact of climate change on sediment load.

Streamflow in Period I was higher than that of Period II, and the mean annual
365 streamflow was 188 and 146 mm.yr⁻¹ for Periods I and II, respectively. Daily flow
duration curves for both periods are displayed in Figure 4. An ANCOVA suggests that
they are significantly different ($p < 0.05$). The $Q_{70\%}$ low flow of the two periods was 2.7
and 2.4 l.s⁻¹, the $Q_{50\%}$ median flow was 4.0 and 3.1 l.s⁻¹, and the $Q_{10\%}$ high flow was
10.7 and 7.5 l.s⁻¹, for the two periods, respectively. The decreased flow regime of
370 Period II, which is probably in part due to an increased evapotranspiration over the
past decades (Duethmann and Blöschl, 2018), indicates that streamflow **cannot**
account for the observed increased sediment load of Period II, otherwise **an increased**
streamflow would be expected **in Period II**.

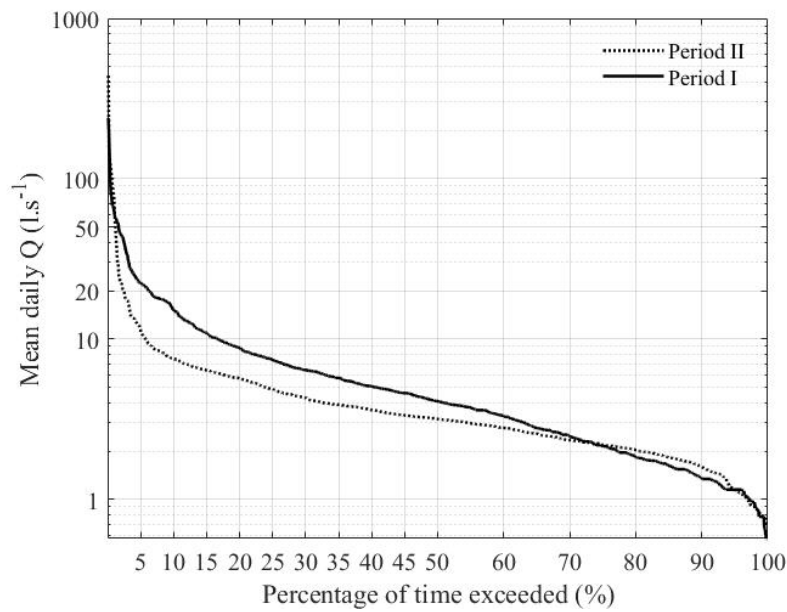


Figure 4 Mean daily flow duration curve for Periods I (solid line) and II (dashed line).

3.2 Change in land use and land organization

Table 1 shows how land use changed between the two periods. During Period I, cropland and grassland accounted for 73% to 82% (varying between years) and 14% to 22%, respectively. However, due to agricultural intensification, cropland increased to around 82% in Period II, at the expense of a decreasing share of grassland. Forest, including sparse forest, accounted for 1.8% area during Period I but increased considerably until Period II to around 11%. The increase in cropland and forest suggest higher rates of evaporation and transpiration, and consequently less streamflow, which is in line with the previously examined trend dynamics of streamflow. When further analyzing the land use classes of arable land, a substantial change was found for the crops types too, with the crops of low risk for soil erosion

390 being replaced with crops that exhibit a high soil loss potential. This was particularly true for maize. In addition, the diversity of crops decreased considerably (Table 2).

This shift towards agricultural uniformity likely acts as a land structure effect. A loss of heterogeneity of crop types increases the probability that different fields are managed with the same crop. Then even smaller fields may behave similar to larger
395 fields in terms of sediment production.

Besides the change in land use, the parcel structure of the catchment has also changed (Table 1). This change was related to a land consolidation plan issued in 1955 in Austria (Devátý et al., 2019) and a massive trend to agricultural industrialization that
400 evolved after 1945 (mainly referring to the massive application of advanced machinery and fertilization technologies that started right in the 1950s). During Period I, arable land was fragmented across many small parcels, with a mean parcel size between 0.5 - 0.6 ha and a parcel density (number of parcels per ha area) between 1.7 - 2.0 ha⁻¹ in different years. In Period II, these values increased considerably to mean
405 parcel sizes between 1.7 - 2.7 ha and parcel densities between 0.3 - 0.6 ha⁻¹. Similarly, the mean parcel size and parcel density of grassland during Period I were 0.13 - 0.17 ha and 5.2 - 7.2 ha⁻¹. It had changed to 1.06 ha and 0.9 ha⁻¹ in Period II. As parcel structures are identified influencing sediment loads mainly due to the boundary effects (e.g. Baudry and Merriam, 1988; Takken et al., 1999; Phillips et al., 2011), the
410 substantial decrease in parcel density and the increase in parcel size of the catchment in Period II, was expected to affect sediment load as well.

Table 1 Parcel and land use statistics for Periods I and II. Land use for the years 1946 to 1949 represents Period I, land use for the years 2007 to 2012 represents Period II; N is the number of parcels for a given land use, density is the number of parcels per ha, mean size represents the mean area of parcels with a particular land use.

Parcel Structure								
Land use	Period I				Period II			
	Parcel number (N)	Density (1·ha ⁻¹)	Mean size (ha)	Area (%)	Parcel number (N)	Density (1·ha ⁻¹)	Mean size (ha)	Area (%)
Arable land	70-111*	1.7-2.0	0.5-0.6	73-82	21-33	0.3-0.6	1.7-2.7	81-82
Grassland	70-81	5.2-7.2	0.1-0.2	14-22	6	0.9	1.1	3-4
Forest	1	-	1.2	1.8	7	1	1.0	10.5-11
Paved area	17	12.9	0.1	2	17	7.3	0.1	2.4

* The number of parcels varied with the specific year of a period

Table 2 Crop statistics of arable land for Periods I and II; Crop statistics for the years 1946 to 1949 represent Period I, crop statistics for the years 2007 to 2012 represent Period II; Erosion risk for a particular crop is classified as high or low according to the classification of management in the RUSLE. The statistical values represent the ranges of the area for each crop during Periods I or II.

Crop	Period I		Period II		Erosion risk
	Area (ha)	Area (%)	Area (ha)	Area (%)	
Meadow	9-15	18-30	0.8	2	low
Alfalfa	11-18	22-33	-	-	low
Wheat	5-14	9-26	3-35	5-66	low
Rye	3-13	5-24			low
Beets	2-12	3-22	-	-	high
Oats	2-10	4-18	2	4	low
Barley	0.3-8	5-15	2-29	5-55	low
Potatoes	3-7	6-14	-	-	high
Maize	0.3-0.8	0.6-1.1	6.3-34	12-63	high
Rape	-	-	0.7-23	1-43	low
Sunflower	-	-	0.2-2	0.3-4	high

3.3 Change in sediment transport regime

3.3.1 Direct comparison of the fitted SRCs

Figure 5 shows the fitted sediment rating curves ($p < 0.05$) for both periods. An

430 ANCOVA suggests that the slopes of the regression lines are significantly ($p < 0.05$) different between the dormant seasons or growing seasons. Although rainfall erosivity of Period II_G was similar to that of Period I_G (Figure 3a) and streamflow of Period II was generally lower than that of Period I (Figure 4), the fitted SRC of Period II_G was steeper than that of Period I_G (Figure 5a), with the coefficients b being 0.3 and 1.6 for Period I_G and Period II_G, respectively (Table 3). The fitted SRC of Period II_D demonstrated a faster response of sediment concentration to increasing flow compared to that of Period I_D (Figure 5b), the coefficients b being 0.8 and 1.7 for Period I_D and Period II_D, respectively. However, the rainfall ED in Period II_D was generally lower than that of Period I_D (Figure 3a), suggesting a lower

440 probability of a substantial increase in sediment availability. These results indicate that neither changes in rainfall erosivity nor the hydrological regime could explain the increase in sediment dynamics.

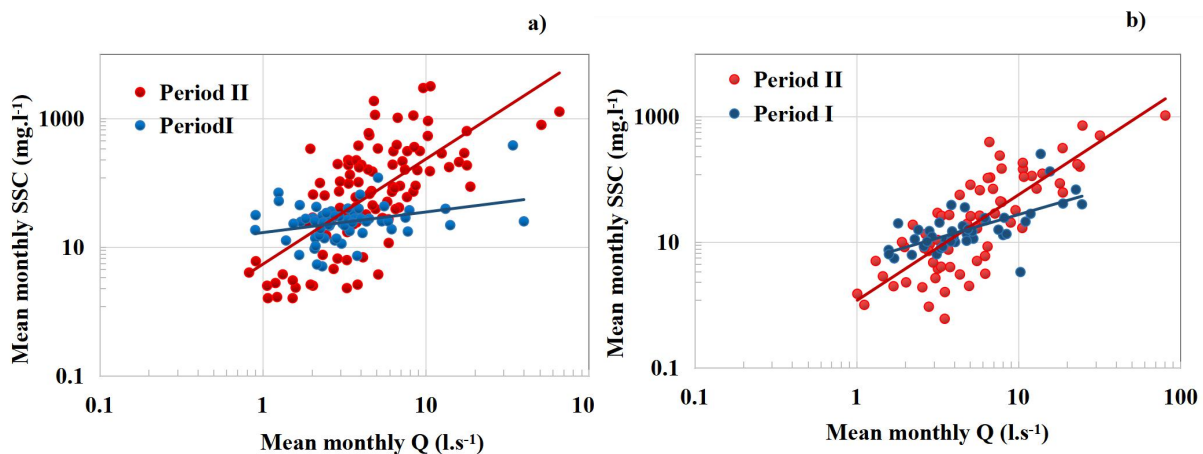


Figure 5 Sediment rating curves for a) the growing seasons and b) the dormant

seasons in the two time periods. Each point represents a monthly mean observation.

Table 3 Parameter values for the coefficients of the SRC for different periods and seasons according to Equation (3).

Period	Coefficient		r^2
	a	b	
Period I_G	16.7	0.3	0.11
Period I_D	4.9	0.8	0.42
Period II_G	5.4	1.6	0.45
Period II_D	1.2	1.7	0.64

3.3.2 Relationship between coefficient a and b

The changing steepness of a fitted SRC does not necessarily imply a change in the sediment regime as the slopes of fitted SRC are sometimes affected by catchment size or the distribution of samples (Asselman, 2000). To minimize possible interference of other factors in identifying variations or shifts of the SRC, we investigated the relationship between coefficients a and b of the SRC. Figure 6 displays the coefficients $\log(a)$ plotted against b for the four investigated time frames.

Interestingly, the data points of both Periods I and II, for the growing season are more concentrated in the right-lower part of the graphs (Figure 6a). A different pattern of $\log(a)$ against b was found for the dormant season (Figure 6b), *i.e.* the data points of Period I concentrated in the right-lower area (blue points), but were more concentrated in the left-upper area for Period II.

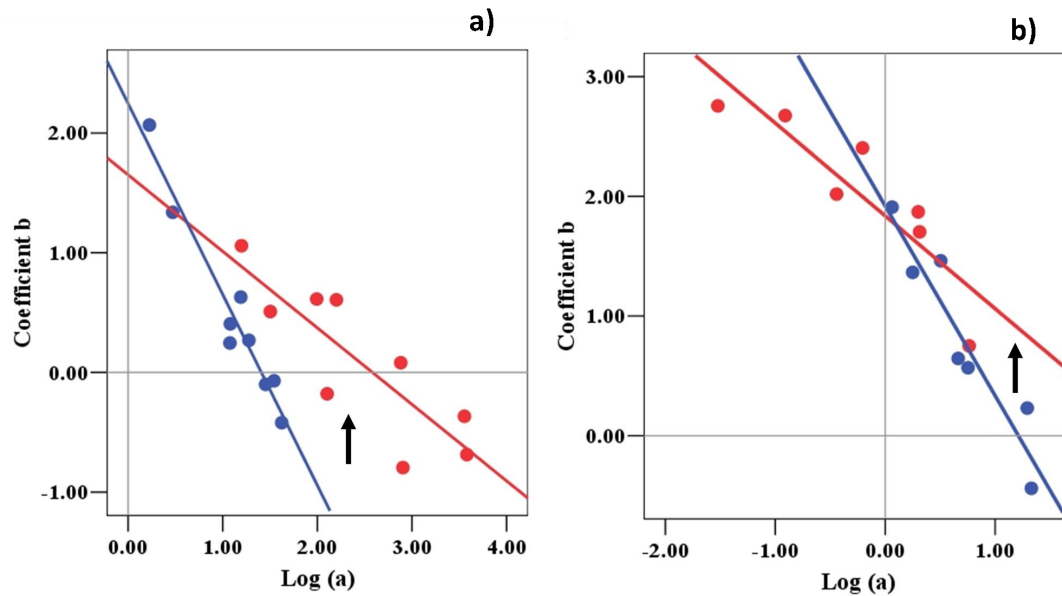


Figure 6 Relationship between coefficients a and b for a) growing season and b) dormant season of Period I (blue) and Period II (red), respectively. $\log(a)$ in x-axis represents the decadal logarithm. The arrows represent sediment regime shifted upward to a certain degree. All regressions are significant at $p < 0.05$.

The regression lines of Periods I to II are different. The intercepts of the regression lines are significantly different ($p < 0.05$) for the growing seasons (Figure 6a). The slopes of the regression lines for Periods I and II were -1.60 and -0.94 in the growing season (Figure 6a), and -1.58 and -0.80 in the dormant season, respectively (Figure 6b). The upward shift of the line at $\log(a)$ larger than around 0.6 suggests that in Period II, most of the sediment was transported at relatively high flow rates. Since climate change was not responsible for the increased hydrological regime (see section 3.1), we mainly attribute this shift to the increase in hydrological connectivity, such as flow path density and flow length, and a change in land use and land cover statistics.

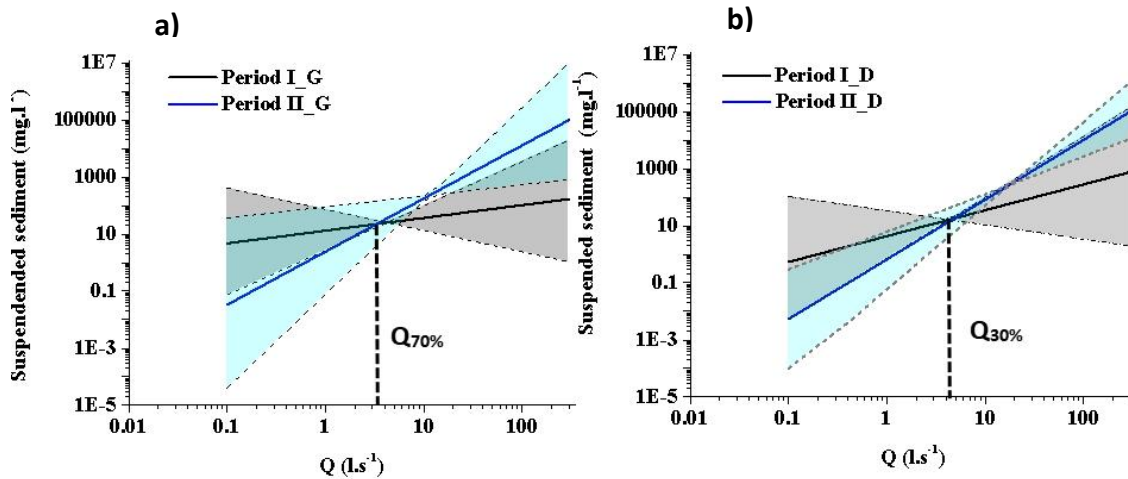


Figure 7 Theoretical sediment rating curves (tSRC) for the growing seasons (a) and the dormant seasons (b) of Period I and II. Solid lines denote the 50 percentile of the tSRC for each period (*i.e.* tSRC_{50%}). The grey area denotes the range of the predicted tSRC composed of 5 and 95 percentiles (*i.e.* tSRC_{5%} and tSRC_{95%}). Q₃₀ % and Q₇₀ % represent the flow conditions of 3.9 l.s⁻¹ and 2.0 l.s⁻¹, respectively.

Figure 7 displays the theoretical sediment rating curves (tSRC) with their uncertainties for the different periods and seasons. ANCOVA suggests that the derived tSRC_{50%} were significantly different ($p < 0.05$) between the two periods, both in the growing seasons and dormant seasons. However, when accounting for uncertainties of the derived tSRCs, the degree of their difference varied with flow rate. Specifically, at a given Q higher than approximately $Q_{70\%}$, sediment concentrations in Period II_G were higher than those in Period I_G (Figure 7a), whereas for flow rates below this value concentrations were not different. This increased sediment transport regime is in line with the observations of the sediment load of Period II_G (6.3 ± 19.9 ton per month) which was significantly higher ($p < 0.05$, t-test) than that of Period I_G (0.8 ± 3.3 ton per month), see Table 4. Sediment concentrations were less different between

the dormant seasons of Period I and Period II at flow rates lower than $Q_{30\%}$. The lack of a statistically significant difference ($p=0.07$) of sediment loads for Period II_D (5.4 ± 18.3 ton per month) and Period I_D (1.3 ± 3.9 ton per month) indicates the difficulty in examining the change in sediment regime for the dormant seasons, but is much less relevant for the annual sediment budget.

Table 4 Monthly mean sediment loads and associated standard deviations of different periods

Period	Growing season ($t \text{ mon}^{-1}$)	Dormant season ($t \text{ mon}^{-1}$)
Period_I	0.8 ± 3.3	1.3 ± 3.9
Period_II	6.3 ± 19.9	5.4 ± 18.3

Note: Estimates based on equation (2)

3.4 Parcel_effect versus LUCC_effect

Figure 8 demonstrates the dynamic contributions of land structure and land cover changes on sediment concentrations with increasing flow. Land consolidation and the substantial increase in cropland at the expense of a decrease in grassland explains the increase in sediment yield. However, the trends of their contributions to this increase differ. Generally, with higher flow rates, the contribution of the LUCC_effect gradually decreased, whilst the contribution of the Parcel_effect increased. The Parcel_effect accounted for more than 50% of the Total_effect after the flow rate exceeded 20 l s^{-1} approximately (*i.e.* $Q_{2\%}$) (Figure 8), exhibiting a dominant role in sediment production. The opposite trend of the contributions between LUCC_effect and Parcel_effect suggests that, even though land consolidation and an increase in cropland both have unbeneficial effects on erosion control, their hydrological consequences may be different, with land structure change probably explaining much of the variation of sediment load at high flow conditions.

Unlike the situation during high flow rates, the Total_effect showed an almost zero value at flow rates less than approximately 2 l.s^{-1} (*i.e.* $Q_{70\%}$), suggesting no difference in sediment load between Periods I and II at low flow conditions. The increase in
525 sediment concentration, at flow rates of 2 up to around 20 l.s^{-1} , seemed to be mainly caused by the increase in the cropland area of Period II, as the contribution from LUCC_effect was consistently higher than that of the Parcel_effect.

One may note that forest cover increased considerably from Period I to Period II. It, however, did not show an influential role in erosion control. We hypothesize that even
530 though a beneficial effect of forest increase (up to a total of 11% of the catchment) may have appeared in Period II, it was easily offset by the negative effect of crop land changes, particularly the increase in row crops. This contributed substantially to sediment yield compared with other land uses and other crop types (Kijowska - Strugała et al., 2018).

535

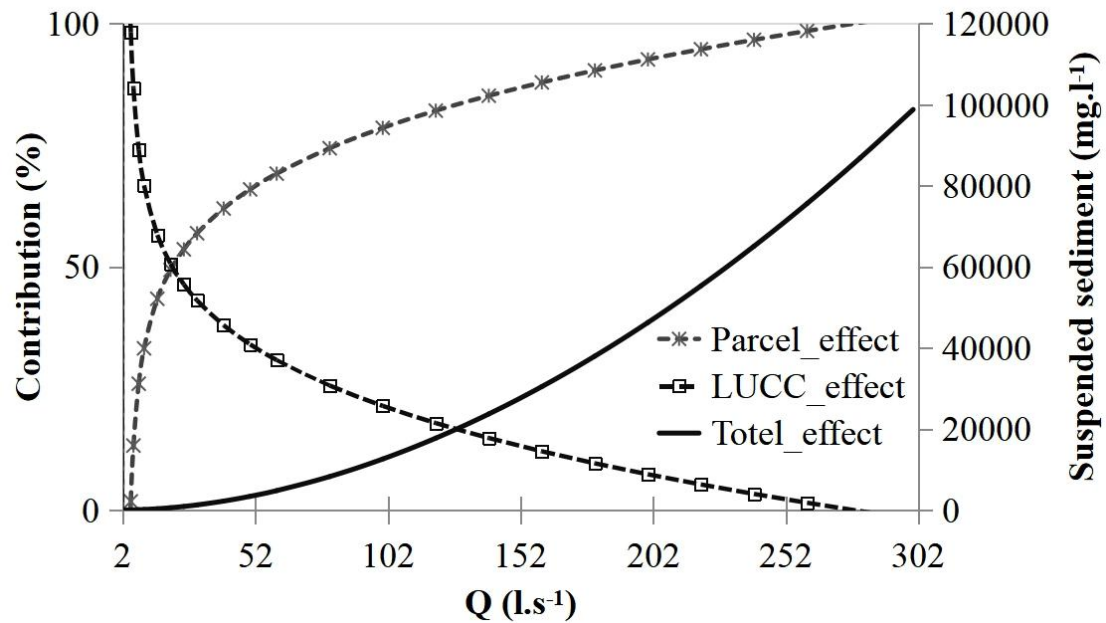


Figure 8 Contribution of Parcel_effect and LUCC_effect to the Total_effect across various flow rates. Total_effect (Equation 4) is displayed in terms of suspended sediment concentration. Parcel_effect and LUCC_effect was estimated by Equations (5) and (6), respectively; their contribution to the Total_effect was estimated by Equations (7) and (8), respectively.

4. Discussion

The industrial intensification of agriculture implemented during the last 70 years has raised considerable concerns regarding erosion and sediment loading of rivers (e.g. Bakker et al., 2008; Chevigny et al., 2014). However, with global climate warming, the different contributions of LUCC, land policy adjustments such as land consolidation, and climate change affecting sediment load remain not well understood.

This paper aims at evaluating the relative roles of climate change, LUCC, and land consolidation in sediment production, particularly at varying flow rates.

4.1 Change in sediment load between two time periods

We found that the sediment load increased almost six fold from Period I to Period II. This finding is supported by estimates of the management factor (C-Factor) and the slope and slope length factor (SL-Factor) of the RUSLE for Period I and Period II (Fiener et al., 2020). While the mean C-Factor of the HOAL catchment increased from 0.16 in Period I to 0.33 in Period II, the SL-Factor increased from 0.76 to 0.96. Added together, the changed values for these two factors increased the theoretical soil loss within the catchment by over 150%. This value is smaller than the changes observed, however it should be noted, that the RUSLE has not been designed to account for sediment loads of catchments but to estimate field scale soil loss within catchments. This may explain the observed differences to a certain extent.

4.2 Potential interference of different sampling methods

Due to technical advancement over the long investigation period, different sampling methods, *i.e.* grab sampling and automatic equal-discharge-increment sampling, were used in this study for Periods I and II, which may affect both rating curve estimation and sediment load estimation (Harmel et al., 2010). Thomas (1988) found that sampling method (random or systematic versus discharge-based sampling), may bias sediment load estimates, but Groten and Johnson (2019) suggested that, for sediment with very fine textural composition, these biases may be small. In our study catchment, the topsoil of the catchment is constituted of 75% silty loam, 20% silty clay loam, and 5% silt according to the USDA soil classification (Pigliafuoco et al., 2019). This very fine soil texture provides confidence to attribute the change in sediment load to internal and/or external driving agents (such as climate, land surface processes),

instead of a methodological discrepancy. In addition, to account for the different sampling frequencies, we employed a relationship of parameter *a* and *b* of the rating curves, which has the merit of not varying with the sampling methods (see section 2.3.2). However, a further study on the effects of sampling methods in future might be shed additional light on the issue.

4.3 Dynamic relevance of land consolidation in controlling sediment load

Climate change in terms of both monthly erosivity density (*ED*) and precipitation (*P*) was not responsible for the increase in sediment load, instead it could be explained by land cover and land consolidation changes. This finding is particularly important in regions, where a strong intensification of agricultural management took place during the last decades. The relative contributions of land cover and land consolidation changes varied with streamflow. For flow conditions below around 5 l.s^{-1} (*i.e.* $Q_{20\%}$), land consolidation had no apparent adverse effect on erosion, but with increasing flow, the contribution to sediment load increased continuously, leading to a dominant role at high flow rates. This finding is partially in line with David et al. (2014) and Cantreul et al. (2020). They reported that landscape structure was less important for soil erosion than land use and land cover during normal flow conditions. However, they did not investigate whether the effect of landscape structure showed a dynamic behavior with increasing flow. In contrast, the LUCC_effect, *i.e.* the increase of crops with high erosion risk, continuously affected sediment load with gradually decreasing importance at high flow conditions. Similar results were reported by Vaughan et al.

(2017), who showed that sediment concentration at low and median flow conditions was considerably associated with a change in catchment characteristics, primarily land use and land cover. Although the role of land use changes was dominating for flow conditions less than $Q_{20\%}$, its contribution to the total annual sediment load was small. More than 75% of the total sediment load was transported during a small number of events (25 events in Period I, 8 events in Period II) and all events had flow rates above 15 l.s^{-1} (approximately at $Q_{13\%}$ in Period I or $Q_{4\%}$ in Period II, respectively), which underlines the importance of land structure for sediment loading.

The dynamic relevance of vegetation and land consolidation in sediment production is associated with the processes and mechanisms controlling overland flow as a transporting agent for sediment (e.g. Sun et al., 2013; El Kateb et al., 2013; Nearing et al., 2017; Silasari et al., 2017; Kijowska - Strugała et al., 2018). A change in land use and land cover implies alterations of surface characteristics, such as above ground structure morphology, litter cover, organic matter components, root network (Gyssels et al., 2005; Wei et al., 2007; Moghadam et al., 2015; Patin et al., 2018) and soil properties (Costa et al., 2003; Moghadam et al., 2015). These properties influence the protective role of vegetation in soil detachment, the flow capacity to transport sediment particles, and runoff flow paths to the stream channels (Van Rompaey et al., 2002; Lana-Renault et al., 2011; Sun et al., 2018). The protective effects tend not to linearly increase with increasing surface runoff. Accelerated discharge and stronger scouring effects of upslope discharge might impair the protective role of vegetation (e.g. Zhang et al., 2011; Santos et al., 2017; Bagagiolo et al., 2018; Yao et al., 2018;

Wang et al., 2019). Vegetation usually exhibits a smaller interception capability at
620 high rainfall intensity, resulting in an enhanced splash erosion and availability of
mobile soil particles (Cayuela et al., 2018; Magliano. et al., 2019; Nytch et al., 2019).
However, the decreasing contribution of the LUCC_effect does not directly imply an
absolute decrease of the magnitude of the LUCC_effect. The absolute change in SSC
resulting from LUCC reveals an increasing trend as flow rates increase. Thus, the
625 contribution of the LUCC_effect stands for the relevance of LUCC in erosion control
compared to the change due to land consolidation. The magnitude of the LUCC_effect
probably depends mainly on where within the catchment the land cover is changed
and how the proportional area of various land uses changes. We will address this topic
in future analyses.

630 Unlike land cover and landuse change, landscape structure is usually combined with
other catchment properties, such as slope characteristics and soil properties
(Gascuel-Oudoux et al., 2011) and additional erosion and transport factors (Verstraeten
et al., 2000), exerting a more complicated influence on erosion. For example, the
effect of landscape structure on soil erosion may be identified on moderate slopes,
635 while on steep slopes it may be concealed by on-site severe soil erosion (Chevigny et
al., 2014). However, the key process for erosion control is the fact that landscape
elements and their structural position (i.e. parcel structure, field boundaries, hedges
and similar) alter hydrological connectivity between land and water. This is
particularly true when the land cover on both sides of boundaries is different (Van
640 Oost et al., 2000). Reducing parcel size and heterogeneity increases hydrological

connectivity significantly and results in a substantial off-site damage effect, irrespective of on-site erosion of the investigated land use (Boardman et al., 2018; Devátý et al., 2019). During low and median flow conditions, surface runoff and sediment may arrive to a lesser extent at field boundaries due to efficient interception effects of the vegetation cover. This may explain the identified dynamic relevance of land structure change in sediment load found here.

5 Conclusions

Climate change, land use and land cover change, and other human-associated activities are widely regarded as potential agents driving hydrological change. Understanding the relevance of each of these agents in the hydrological cycle is critical for implementing adaptive catchment management measures and addressing climate change. Although very significant climate change influences in the last decades have been identified for certain components of the hydrological cycle we found that climate change expressed in changes in rainfall erosivity and precipitation cannot explain the increased sediment production between 1946-1954 and 2002-2017 in the investigated catchment. Instead, both land cover and land consolidation played important, dynamic roles in erosion and sediment production.

The relevance of land use and land cover change versus land consolidation change varied dynamically with changing flow conditions. The reduction in parcel density undoubtedly increased sediment load, particularly at higher flows due to the decreased capacity of trapping sediment particles between parcels and increasing flow lengths

inside parcels. Unfavorable land use or land cover change increased sediment load at most flow conditions, although the relevance of this process decreases at high or very high flow rates. Therefore, when addressing soil conservation measures at the catchment scale, the distribution of fields, land structure, and vegetation cover should be simultaneously considered. Such a strategy would be conducive to dealing with the risk of soil erosions at different flow rates. Land use policy adjustments resulting from technological development have been vital to deal with food security issues in the past. However, now we experience the negative influence of these adjustments on the hydrological cycle. Therefore, rather than focusing on climate change solely, we need to pay increased attention to anthropic management activities to counteract their negative impact on hydrological change effectively.

Author contributions

Shengping Wang has led the data analysis, drafted the manuscript, and revised the manuscript; Peter Strauss was responsible for the project design, oversaw the whole analysis, and conducted manuscript revision as the project leader; Carmen Krammer was responsible for data collection and data preparation; Elmar Schmaltz contributed to figure drawing and manuscript revision; Borbala Szeles has helped to revise the manuscript, and Günter Blöschl oversaw and critically reflected on the manuscript writing as the senior scientist.

Competing interests

The authors declare that they have no conflict of interest.

Disclaimer

Publisher's note: Copernicus Publications remains neutral with regard to jurisdictional
690 claims in published maps and institutional affiliations.

Acknowledgements

This work is financially supported by the SHUI project (Soil Hydrology research
platform underpinning innovation to manage water scarcity in European and Chinese
695 cropping systems) within the Horizon 2020 Research and Innovation Action of the
European Community (No. 773903), the Austrian Science Funds (FWF), project
W1219-N28, and the TU Wien Risk network.

References

- 700 Asselman, N. E. M.: Fitting and interpretation of sediment rating curves, *Journal of Hydrology*,
234(3-4), 228-248, [https://doi.org/10.1016/S0022-1694\(00\)00253-5](https://doi.org/10.1016/S0022-1694(00)00253-5), 2000.
- Awal, R., Sapkota, P., Chitrakar, S., Thapa, B. S., Neopane, H. P., & Thapa, B.: A General Review
on Methods of Sediment Sampling and Mineral Content Analysis, *Journal of Physics: Conference*
Series, 1266(1), <https://doi.org/10.1088/1742-6596/1266/1/012005>, 2019
- 705 Bagagiolo, G., Biddoccu, M., Rabino, D., Cavallo, E.: Effects of rows arrangement, soil
management, and rainfall characteristics on water and soil losses in Italian sloping vineyards,
Environmental Research, 166, 690-704, 2018
- Bakker, M., Govers, G., van Doorn, A., Quetier, F., Chouvardas, D., Rounsevell, M.: The response
of soil erosion and sediment export to land-use change in four areas of Europe: The importance of
710 landscape pattern, *Geomorphology*, 98, 213-226, 2008.
- Baudry, J. and Merriam, H.G.: Connectivity in landscape ecology, in: *Proc. 2nd Intern. Semin. of*
IALE, Muenster 1987. *Muensterische Geographische Arbeiten* 29, 23-28, 1988
- Bellin, N., Vanacker, V., De Baets, S.: Anthropogenic and climatic impact on Holocene sediment
dynamics in SE Spain: A review, *Quaternary International*, 308-309, 112-129, 2013
- 715 Bochet, E., Poesen, J., Rubio, J.L.: Runoff and soil loss under individual plants of a semi-arid
Mediterranean shrubland: influence of plant morphology and rainfall intensity, *Earth Surf. Process.*
Landforms, 31, 536-549, 2006.

- Bouma, J., Varallyay, G., Batjes, N.H.: Principal land use changes anticipated in Europe. *Agr. Ecosyst. Environ.*, 67 (2-3), 103-119, 1998.
- 720 Blöschl, G., Blaschke, A. P., Broer, M., Bucher, C., Carr, G., Chen, X., Eder, A., Exner-Kittridge, M., Farnleitner, A., Flores-Orozco, A., Haas, P., Hogan, P., KazemiAmiri, A., Oismüller, M., Parajka, J., Silasari, R., Stadler, P., Strauss, P., Vreugdenhil, M., Wagner, W., and Zessner, M.: The Hydrological Open Air Laboratory (HOAL) in Petzenkirchen: a hypothesis-driven observatory, *Hydrol. Earth Syst. Sci.*, 20, 227-255, doi:10.5194/hess-20-227-2016, 2016.
- 725 Cantreul, V., Pineux, N., Swerts, G., Biielders, C., Degré, A.: Performance of the LandSoil expert-based model to map erosion and sedimentation: application to a cultivated catchment in central Belgium, *Earth Surf. Process. Landforms*, DOI: 10.1002/esp.4808, 2020
- Cayuela, C., Llorens, P., Sanchez-Costa, E., Levia, D.F., Latron, J.: Effect of biotic and abiotic factors on inter- and intra-event variability in stemflow rates in oak and pine stands in a Mediterranean mountain area, *Journal of Hydrology*, 560: 396-406, 2018.
- 730 Chevigny, E., Quiquerez, A., Petit, C., Curmi, P.: Lithology, landscape structure and management practice changes: Key factors patterning vineyard soil erosion at metre-scale spatial resolution, *CATENA*, 121, 354-364, 2014.
- Costa, M.H., Botta, A., Cardille, J.A.: Effects of large scale changes in land cover on the discharge of the Tocantins River, Southeastern Amazonia, *Journal of Hydrology*, 283, 206-217, 2003.
- 735 David, M., Follain, S., Ciampalini, R., Le Bissonnais, Y., Couturier, A., Walter, C.: Simulation of medium-term soil redistributions for different land use and landscape design scenarios within a vineyard landscape in Mediterranean France, *Geomorphology*, 214, 10-21, 2014.
- Desilets, S.L.E., Nijssen, B., Ekwurzel, B., Ferre, T.P.A.: Post-wildfire changes in suspended sediment rating curves: Sabino Canyon, Arizona, *Hydrol. Process.*, 21, 1413-1423, 2007
- 740 Devátý, J., Dostál, T., Hösl, R., Krása, J., Strauss, P.: Effects of historical land use and land pattern changes on soil erosion - Case studies from Lower Austria and Central Bohemia, *Land Use Policy*, 82, 674-685, <https://doi.org/10.1016/j.landusepol.2018.11.058>, 2019
- Duethmann, D., and Blöschl, G.: Why has catchment evaporation increased in the past 40 years? A data-based study in Austria. *Hydrology and Earth System Sciences*, 22, 5143-5158, <https://doi.org/10.5194/hess-22-5143-2018>, 2018.
- 745

- Eder, A., Exner-Kittridge, M., Strauss, P., Blöschl, G.: Re-suspension of bed sediment in a small stream – results from two flushing experiments, *Hydrology and Earth System Sciences*, 18, 1043–1052, 2014
- 750 El Kateb, H., Zhang, H.F., Zhang, P.C., Mosandl, R.: Soil erosion and surface runoff on different vegetation covers and slope gradients: A field experiment in Southern Shaanxi Province, China, *CATENA*, 105, 1–10, 2013
- Fan, X., Shi, C., Zhou, Y., Shao, W. : Sediment rating curves in the Ningxia-Inner Mongolia reaches of the upper Yellow River and their implications, *Quaternary International*, 282, 152–162, <https://doi.org/10.1016/j.quaint.2012.04.044>, 2012
- 755 152–162, <https://doi.org/10.1016/j.quaint.2012.04.044>, 2012
- Fiener, P., Dostal, T., Krasa, J., Schmaltz, E., Strauss, P., and Wilken, F.: Operational USLE-Based Modelling of Soil Erosion in Czech Republic, Austria, and Bavaria – Differences in Model Adaptation, Parametrization, and Data Availability, *Applied Sciences*, 10, 3647, 1–18, Doi:10.3390/app10103647, 2020.
- 760 García-Ruiz, J. M.: The effects of land uses on soil erosion in Spain?: A review, *CATENA*, 81(1), 1–11, <https://doi.org/10.1016/j.catena.2010.01.001>, 2010.
- Gascuel-Oudou, C., Aurousseau, P., Doray, T., Squvidant, H., Macary, F., Uny, D., Grimaldi, C. : Incorporating landscape features to obtain an object-oriented landscape drainage network representing the connectivity of surface flow pathways over rural catchments, *Hydrological Processes*, 25(23), 3625–3636, 2011.
- 765 3625–3636, 2011.
- Groten, J. T., & Johnson, G. D.: Comparability of river suspended-sediment sampling and laboratory analysis methods, *Scientific Investigations Report*, 1–23, 2018.
- Guzman, C. D., Tilahun, S. A., Zegeye, A. D., Steenhuis, T. S.: Suspended sediment concentration-discharge relationships in the (sub-) humid Ethiopian highlands, *Hydrology and Earth System Sciences*, 17(3), 1067–1077, <https://doi.org/10.5194/hess-17-1067-2013>, 2013.
- 770 1067–1077, <https://doi.org/10.5194/hess-17-1067-2013>, 2013.
- Gyssels, G., Poesen, J., Bochet, E., Li, Y.: Impact of plant roots on the resistance of soils to erosion by water: a review, *Prog. Phys. Geogr.*, 29, 189–217, 2005.
- Harmel, R. D., Slade, R. M., & Haney, R. L.: Impact of Sampling Techniques on Measured Stormwater Quality Data for Small Streams, *Journal of Environmental Quality*, 39(5), 1734–1742, <https://doi.org/10.2134/jeq2009.0498>, 2010.
- 775 1734–1742, <https://doi.org/10.2134/jeq2009.0498>, 2010.
- Haslinger, K., Hofstätter, M., Kroisleitner, C., Schöner, W., Laaha, G., Holawe, F., & Blöschl, G. : Disentangling Drivers of Meteorological Droughts in the European Greater Alpine Region

- During the Last Two Centuries, *Journal of Geophysical Research: Atmospheres*, 124(23), 12404–12425, <https://doi.org/10.1029/2018JD029527>, 2019.
- 780 Hou, J., Zhu, H., Fu, B., Lu, Y., Zhou, J.: Functional traits explain seasonal variation effects of plant communities on soil erosion in semiarid grasslands in the Loess Plateau of China, *CATENA*, 194, 104743, <https://doi.org/10.1016/j.catena.2020.104743>, 2020.
- Hu, B., Wang, H., Yang, Z., & Sun, X.: Temporal and spatial variations of sediment rating curves in the Changjiang (Yangtze River) basin and their implications, *Quaternary International*, 230(1–2), 785 34–43, <https://doi.org/10.1016/j.quaint.2009.08.018>, 2011.
- IUSS Working Group WRB, World Reference Base for Soil Resources 2014, update 2015 International soil classification system for naming soils and creating legends for soil maps, World Soil Resources Reports No. 106. FAO, Rome, 2015.
- Kelly, C.N., Mc Guire, K.J., Miniati, C.F., Vose, J.M.: Streamflow response to increasing 790 precipitation extremes altered by forest management. *Geophys. Res. Lett.* 43(8), 3727–3736, <https://doi.org/10.1002/2016GL068058>, 2016.
- Khaledian, H., Faghih, H., Amini, A.: Classifications of runoff and sediment data to improve the rating curve method. *Journal of Agricultural Engineering*, 48(3), 147–153, <https://doi.org/10.4081/jae.2017.641>, 2017.
- 795 Kijowska - Strugata, M., Bucala - Hrabia, A., Demczuk, P.: Long-term impact of land use changes on soil erosion in an agricultural catchment (in the Western Polish Carpathians), *Land Degrad. Dev.*, 29, 1871–1884, 2018.
- Korkanç, S. Y.: Effects of the land use/cover on the surface runoff and soil loss in the Niğde-Akkaya Dam Watershed, Turkey, *CATENA*, 163:233–243, 800 <https://doi.org/10.1016/j.catena.2017.12.023>, 2018.
- Kottek, M., Grieser J., Beck, C., Rudolf, B., Rubel, F.: World Map of the Köppen-Geiger climate classification updated. *Meteorol. Z.*, 15, 259–263. DOI: 10.1127/0941-2948/2006/0130, 2006.
- Kundzewicz, Z.W. (Ed.): *Changes in Flood Risk in Europe*. IAHS Special Publication 10, 516 pp, 2012.
- 805 Lana-Renault, N., Latron, J., Karssenbergh, D., Serrano-Muela, P., Reguees, D., Bierkens, M. F. P.: Differences in stream flow in relation to changes in land cover: A comparative study in two sub-Mediterranean mountain catchments, *Journal of Hydrology*, 411(3–4), 366–378, 2011.
- Li, S., Bing, Z., Jin, G.: Spatially explicit mapping of soil conservation service in monetary units

- due to land use/cover change for the three gorges reservoir area, China. *Remote Sensing*, 11(4), 6-8, <https://doi.org/10.3390/rs11040468>, 2019.
- Li, Y., Li, J.J., Are, K. S., Huang, Z.G., Yu, H. Q., Zhang, Q.W.: Livestock grazing significantly accelerates soil erosion more than climate change in Qinghai-Tibet Plateau: Evidenced from ¹³⁷Cs and ²¹⁰Pbex measurements, *Agriculture, Ecosystems & Environment*, 285, doi:10.1016/j.agee.2019.106643, 2019.
- Madarász, B., Jakab, G., Szalai, Z., Juhos, K., Kotroczó, Z., Tóth, A., Ladányi, M.: Long-term effects of conservation tillage on soil erosion in Central Europe: A random forest-based approach, *Soil and Tillage Research*, 209, <https://doi.org/10.1016/j.still.2021.104959>, 2021.
- Madsen, H., Lawrence, D., Lang, M., Martinkova, M., Kjeldsen, T. R.: Review of trend analysis and climate change projections of extreme precipitation and floods in Europe, *Journal of Hydrology*, 519, 3634–3650, <https://doi.org/10.1016/j.jhydrol.2014.11.003>, 2014.
- Magliano, Patricio N., Whitworth-Hulse, Juan, I., Florio, Eva L., Aguirre, E.C., Blanco, L.J.: Interception loss, throughfall and stemflow by *Larreadivaticata*: The role of rainfall characteristics and plant morphological attributes, *Ecological Research*, 34(6), 753-764, 2019.
- Merriam, G.: Ecological processes in the time and space farmland mosaics, in: *Changing Landscapes: An Ecological Perspective*. 286 pp. Edited by S. Zonneveld and R.T.T. Forman, Springer-Verlag, New-York, pp. 121-126, 1990.
- Moghadam, B., Jabarifar, M., Bagheri, M., Shahbazi, E.: Effects of land use change on soil splash erosion in the semi-arid region of Iran, *Geoderma*, 241-242, 210-220, 2015.
- Moravcová, J., Koupilová, M., Pavlíček, T., Zemek, F., Kvítek, T., Pečenka, J.: Analysis of land consolidation projects and their impact on land use change, landscape structure, and agricultural land resource protection: case studies of Pilsen-South and Pilsen-North (Czech Republic), *Landscape and Ecological Engineering*, 13(1), 1-13, <https://doi.org/10.1007/s11355-015-0286-y>, 2017.
- Mullan, Donall.: Soil erosion under the impacts of future climate change: Assessing the statistical significance of future changes and the potential on-site and off-site problems, *CATENA*, 109, 234-246, 2013.
- Nampak, H., Pradhan, B., MojaddadiRizeei, H., Park, H. J.: Assessment of land cover and land use change impact on soil loss in a tropical catchment by using multitemporal SPOT-5 satellite images and Revised Universal Soil Loss Equation model, *Land Degradation and Development*, 29(10), 3440-3455, <https://doi.org/10.1002/ldr.3112>, 2018.

- Nearing, M. A., Pruski, F. F., O'Neal, M. R.: Expected climate change impacts on soil erosion rates: A review, *Journal of Soil and Water Conservation*, 59 (1), 43-50, 2004.
- Nearing, M. A., Xie, Y., Liu, B., Ye, Y.: Natural and anthropogenic rates of soil erosion, *International Soil and Water Conservation Research*, 5, 77-84,
845 <https://doi.org/10.1016/j.iswcr.2017.04.001>, 2017.
- Nytch, C. J., Melendez-Ackerman, E. J., Perez, M., Ortiz-Zayas J.R.: Rainfall interception by six urban trees in San Juan, Puerto Rico, *Urban Ecosystems*, 22(1), 103-115, 2019.
- Palazon, L., Navas, A.: Land use sediment production response under different climatic conditions in an alpine–prealpine catchment, *CATENA*, 137, 244-255, 2016.
- 850 Patin, J., Mouche, E., Ribolzi, O., Sengtahevong, O., Latsachak, K.O., Soulileuth, B., Chaplot, V., Valentin, C.: Effect of land use on interrill erosion in a montane catchment of Northern Laos: An analysis based on a pluri-annual runoff and soil loss database, *Journal of Hydrology*, 563, 480-494, 2018.
- Perović, V., Jakšić, D., Jaramaz, D., Koković, N., Čakmak, D., Mitrović, M., Pavlović,
855 P.: Spatio-temporal analysis of land use/land cover change and its effects on soil erosion (Case study in the Oplenac wine-producing area, Serbia), *Environmental Monitoring and Assessment*, 190 (11), <https://doi.org/10.1007/s10661-018-7025-4>, 2018.
- Phillips, R. W., Spence, C., & Pomeroy, J. W.: Connectivity and runoff dynamics in heterogeneous basins, *Hydrological Processes*, 25(19), 3061-3075, <https://doi.org/10.1002/hyp.8123>, 2011.
- 860 Picciafuoco, T., Morbidelli, R., Flammini, A., Saltalippi, C., Corradini, C., Strauss, P., & Blöschl, G.: A Pedotransfer Function for Field - Scale Saturated Hydraulic Conductivity of a Small Watershed, *Vadose Zone Journal*, 18(1), 1–15, <https://doi.org/10.2136/vzj2019.02.0018>, 2019
- Prosdocimi, M., Cerdà, A., Tarolli, P.: Soil water erosion on Mediterranean vineyards: A review, *CATENA*, 141, 1-21, <https://doi.org/10.1016/j.catena.2016.02.010>, 2016.
- 865 Salesa, D., & Cerdà, A.: Soil erosion on mountain trails as a consequence of recreational activities. A comprehensive review of the scientific literature, *Journal of Environmental Management*, 271, <https://doi.org/10.1016/j.jenvman.2020.110990>, 2020.
- Santos, J.C.N., de Andrade, E.M., Medeiros, P.H.A., Guerreiro, M.J.S., Palacio, H.A.D.: Effect of Rainfall Characteristics on Runoff and Water Erosion for Different Land Uses in a Tropical
870 Semiarid Region, *Water Resources Management*, 31(1), 173-185, 2017.
- Scholz, G., Quinton, J.N., Strauss, P.: Soil erosion from sugar beet in Central Europe in response to

- climate change induced seasonal precipitation variations, *CATENA*, 72, 91–105,
<https://doi.org/10.1016/j.catena.2007.04.005>, 2008.
- Sharma, A., Tiwari, K. N., Bhadoria, P. B. S.: Effect of land use land cover change on soil erosion
 875 potential in an agricultural watershed, *Environmental Monitoring and Assessment*, 173(1-4),
 789-801, <https://doi.org/10.1007/s10661-010-1423-6>, 2011.
- Sheridan, G. J., Lane, P. N. J., Sherwin, C. B., Noske, P. J.: Post-fire changes in sediment rating
 curves in a wet Eucalyptus forest in SE Australia, *Journal of Hydrology*, 409(1-2), 183-195,
<https://doi.org/10.1016/j.jhydrol.2011.08.016>, 2011.
- 880 Silasari, R., Parajka, J., Ressler, C., Strauss, P., and Blöschl. G.: Potential of time-lapse photography
 for identifying saturation area dynamics on agricultural hillslopes, *Hydrological Processes*, 31,
 3610–3627, doi: 10.1002/hyp.11272, 2017.
- Smakhtin, V.U.: Low flow hydrology: a review, *Journal of Hydrology*, 240 (3-4), 147-186, 2001.
- Syvitski, J.P., Morehead, M.D., Bahr, D.B., Mulder, T.: Estimating fluvial sediment transport: the
 885 rating parameters, *Water Resour. Res.*, 36 (9), 2747-2760, 2000.
- Sun, D., Yang, H., Guan, D., Yang, M., Wu, J.B., Yuan, F.H., Jin, C.J., Wang, A.Z., Zhang,
 Y.S.: The effects of land use change on soil infiltration capacity in China: A meta-analysis, *Science
 of the Total Environment*, 626, 1394-1401, 2018.
- Sun, P.C., Wu, Y.P., Wei, X.H., Sivakumar, B., Qiu, L.J., Mu, X.M., Chen, J., Gao, J.E.:
 890 Quantifying the contributions of climate variation, land use change, and engineering measures for
 dramatic reduction in streamflow and sediment in a typical loess watershed, China, *Ecological
 engineering*, 142, <https://doi.org/10.1016/j.ecoleng.2019.105611>, 2020.
- Sun, W.Y., Shao, Q.Q., Liu, J.Y.: Soil erosion and its response to the changes of precipitation and
 vegetation cover on the Loess Plateau, *JOURNAL OF GEOGRAPHICAL SCIENCES*,
 895 23(6), 1091-1106, 2013.
- Syvitski, J.P.M., Alcott, J.M.: RIVER3: simulation of water and sediment river discharge from
 climate and drainage basin variables, *Comput. Geosci.*, 21, 89-151, 1995.
- Takken, I., Beuselinck, L., Nachtergaele, J., Govers, G., Poesen, J., Degraer, G.: Spatial evaluation
 of a physically-based distributed erosion model (LISEM), *CATENA*, 37, 431-447, 1999.
- 900 Tang, C., Liu, Y., Li, Z., Guo, L., Xu, A., Zhao, J.: Effectiveness of vegetation cover pattern on
 regulating soil erosion and runoff generation in red soil environment, southern China, *Ecological
 Indicators*, 129, 107956, <https://doi.org/10.1016/j.ecolind.2021.107956>, 2021.

Thomas, R. B.: Monitoring baseline suspended sediment in forested basins: the effects of sampling on suspended sediment rating curves, *Hydrological Sciences Journal*, 33,5- 10, 1988.

905 USDA-Staff. 2019. Rainfall intensity summarisation tool (RIST) in:
<https://www.ars.usda.gov/southeast-area/oxford-ms/national-sedimentation-laboratory/watershed-physical-processes-research/research/rist> (Accessed in January, 2020)

Van Oost, K., Govers, G., Desmet, P.: Evaluating the effects of changes in landscape structure on soil erosion by water and tillage, *Landscape Ecology*, 15(6), 577-589,
910 <https://doi.org/10.1023/A:1008198215674>, 2000.

Vaughan, A. A., Belmont, P., Hawkins, C. P., Wilcock, P. : Near-Channel Versus Watershed Controls on Sediment Rating Curves, *Journal of Geophysical Research: Earth Surface*, 122(10), 1901-1923, <https://doi.org/10.1002/2016JF004180>, 2017.

Vanmaercke, M., Zenebe, A., Poesen, J., Nyssen, J., Vertstraeten, G., and Deckers, J.:Sediment
915 dynamics and the role of flash floods in sediment export from medium-sized catchments: a case study from the semi-arid tropical highlands in northern Ethiopia, *J. Soil. Sediment.*, 10, 611-627, 2010.

Van Rompaey, A.J.J., Verstraeten, G., van Oost, K., Govers, G., Poesen, J.: Modelling mean annual sediment yield using a distributed approach, *Earth Surface Processes and Landforms*,
920 26,1221-1236, 2002.

Wang, J., Shi, X., Li, Z., Zhang, Y., Liu, Y., Peng, Y.:Responses of runoff and soil erosion to planting pattern, row direction, and straw mulching on sloped farmland in the corn belt of northeast China, *Agricultural Water Management*, 253(December 2020), 106935,
<https://doi.org/10.1016/j.agwat.2021.106935>, 2021

925 Wang, L.J., Zhang, G.H., Wang, X., Li, X.Y.:Hydraulics of overland flow influenced by litter incorporation under extreme rainfall, *Hydrological Processes*, 33(5), 737-747, 2019.

Wang, S.P., McVicar, Tim R., Zhang, Z.Q., Brunner, T., Strauss, P. : Globally partitioning the simultaneous impacts of climate-induced and human-induced changes on catchment streamflow: A review and meta-analysis, *Journal of Hydrology*, <https://doi.org/10.1016/j.jhydrol.2020.125387>,
930 2020.

Warrick, J.A., Rubin, D. M.:Suspended-sediment rating curve response to suburbanization and wildfire, Santa Ana River, California, *Journal of Geophysical Research*, 112, F02018, doi:10.1029/2006JF000662, 2007.

- Wei, W., Chen, L., Fu, B., Huang, Z., Wu, D., Gui, L.: The effect of land uses and rainfall regimes
935 on runoff and soil erosion in the semi-arid loess hilly area, China, *Journal of Hydrology*, 335,
247-258, 2007.
- Yao, J.J., Cheng, J.H., Zhou, Z.D., Sun, L., Zhang, H.J.: Effects of herbaceous vegetation coverage
and rainfall intensity on splash characteristics in northern China, *CATENA*, 167, 411-421, 2018.
- Zhang, G.H., Liu, G.B., Wang, G.L., Wang, Y.X.: Effects of vegetation cover and rainfall intensity
940 on sediment-associated nitrogen and phosphorus losses and particle size composition on the Loess
Plateau, *Journal of Soil and Water Conservation*, 66(3), 192-200, 2011.
- Zhang, X.A., She, D., L., Hou, M., T., Wang, G.B., Liu, Y.: Understanding the influencing factors
(precipitation variation, land use changes and check dams) and mechanisms controlling changes in
the sediment load of a typical Loess watershed, China, *Ecological Engineering*, 163,
945 <https://doi.org/10.1016/j.ecoleng.2021.106198>, 2021.
- Zhang, X.C., Nearing, M.A.: Impact of climate change on soil erosion, runoff, and wheat
productivity in central Oklahoma, *CATENA*, 61, 185-195, 2005.
- Zhang, Y., Xu, C., & Xia, M.: Can land consolidation reduce the soil erosion of agricultural land in
hilly areas? Evidence from Lishui district, Nanjing city, *Land*, 10(5),
950 <https://doi.org/10.3390/land10050502>, 2021.